membrane fusion at temperatures where the membrane remains in the bilayer phase. Thus, despite of their similar structure, the two diolein isomers affect membrane phase behavior and vesicle fusion and leakage rates to different extents. These properties are likely altered by changes in the physical properties of the membranes. Thus, 1,2-diolein is more effective in destabilizing bilayers than is the 1,3-isomer. This may contribute to its greater ability to activate PKC.

Registry No. *N*-Methyl-DOPE, 96687-23-9; 1,2-diolein, 2442-61-7; 1,3-diolein, 2465-32-9; eicosane, 112-95-8.

REFERENCES

Allen, B. G., & Katz, S. (1991) *Biochemistry 30*, 4334-4343.

Bentz, J., Nir, S., & Wilschut, J. (1983) *Colloids Surf. 6*, 333-363.

Boni, L. T., & Rando, R. R. (1985) *J. Biol. Chem. 260*, 10819-10825.

Cullis, P. R., & de Kruijff, B. (1978) *Biochim. Biophys. Acta 513*, 31-42.

Ellens, H., Siegel, D. P., Alford, D., Yeagle, P. L., Boni, L., Lis, L. J., Quinn, P. J., & Bentz, J. (1989) *Biochemistry 28*, 3692-3703.

Epand, R. M., & Lester, D. S. (1990) *Trends Pharmacol. Sci. 11*, 317-320.

Epand, R. M., Stafford, A. R., Cheetham, J. J., Bottega, R., & Ball, E. H. (1988) *Biosci. Rep. 8*, 49-54.

Epand, R. M., Epand, R. F., & Lancaster, C. R. D. (1989) *Biochim. Biophys. Acta 945*, 161-166.

Gagne, J., Stamatatos, J., Diacovo, T., Hui, S. W., Yeagle, P. L., & Silvius, J. R. (1985) *Biochemistry 24*, 4400-4408.

Gómez-Fernández, J. C., Aranda, F. J., Villalain, J., Micol, V., Ortiz, A., & Hernández, T. (1990) in *Horizons in Membrane Biotechnology* (Nicolau, C., & Chapman, D., Eds.) pp 53-67, Wiley-Liss, New York.

Gruner, S. M. (1985) *Proc. Natl. Acad. Sci. U.S.A. 82*, 3665-3669.

Gruner, S. M., Tate, M. W., Kirk, G. L., So, P. T. C., Turner, D. C., Keane, D. T., Tilcock, C. P. S., & Cullis, P. R. (1988) *Biochemistry 27*, 2853-2866.

Hamilton, J. A., Bhamidipati, S. P., Kodali, D. R., & Small, D. H. (1991a) *J. Biol. Chem. 266*, 1177-1186.

Hamilton, J. A., Fujito, D. T., & Hammer, C. F. (1991b) *Biochemistry 30*, 2894-2902.

Kelsey, D. R., Flanagan, T. D., Young, J. E., & Yeagle, P. L. (1991) *Virology 182*, 690-702.

Kodali, R. D., Tercyak, A., Fahey, D. A., & Small, D. M. (1990) *Chem. Phys. Lipids 52*, 163-170.

Micol, V., Aranda, F. J., Villalain, J., & Gómez-Fernández, J. C. (1990) *Biochem. Int. 20*, 957-965.

Molleyres, L. P., & Rando, R. R. (1988) *J. Biol. Chem. 263*, 14832-14838.

Nishizuka, Y. (1986) *Science 233*, 305-312.

Siegel, D. P., & Banschbach, J. L. (1990) *Biochemistry 29*, 5975-5981.

Siegel, D. P., Banschbach, J., Alford, D., Ellens, H., Lis, L., Quinn, P. J., Yeagle, P. L., & Bentz, J. (1989a) *Biochemistry 28*, 3703-3709.

Siegel, D. P., Banschbach, J., & Yeagle, P. L. (1989b) *Biochemistry 28*, 5010-5019.

Siegel, D. P., Burns, J. L., Chestnut, M. H., & Talmon, Y. (1989c) *Biophys. J. 56*, 161-169.

Sternin, E. (1988) Ph.D. Thesis, Department of Physics, University of British Columbia, Vancouver, Canada.

Struck, D., Hoekstra, D., & Pagano, R. E. (1981) *Biochemistry 20*, 4093-4099.

Structure of Epidermal Growth Factor Bound to Perdeuterated Dodecylphosphocholine Micelles Determined by Two-Dimensional NMR and Simulated Annealing Calculations†

Daisuke Kohda and Fuyuhiko Inagaki*

Department of Molecular Physiology, the Tokyo Metropolitan Institute of Medical Science, 18-22 Honkomagome 3-chome, Bunkyo-ku, Tokyo 113, Japan

Received August 5, 1991; Revised Manuscript Received October 16, 1991

ABSTRACT: The interaction of mouse epidermal growth factor (mEGF) with micelles of a phospholipid analogue, perdeuterated dodecylphosphocholine (DPC), was investigated by two-dimensional ^{1}H NMR. Sequence-specific resonance assignments of the micelle-bound mEGF have been made, and the chemical shifts were compared with those in the absence of DPC. DPC induced large chemical shift changes of the resonances from the residues in the C-terminal tail (residues 46-53) but little perturbation on the residues in the main core (residues 1-45). Starting from the three-dimensional structure in the absence of DPC, micelle-bound structures were calculated using the program XPLOR with interproton distance data obtained from NOESY spectra recorded in the presence of DPC. The C-terminal tail of mEGF was found to change conformation to form an amphiphilic structure when bound to the micelles. It is possible that induced fit in the C-terminal tail of mEGF occurs upon binding to a putative hydrophobic pocket of the EGF receptor.

Micellar systems have long been used as models for membranes. They are superior to organic solvent systems, such as methanol and trifluoroethanol, since they can mimic the lipid-water interface as well as the hydrophobic environment. In the field of ^{1}H NMR, the conformations of peptides bound to micelles have been investigated as a model of membrane-bound forms (Brown et al., 1982; Braun et al., 1983; Olejniczak et al., 1988; Inagaki et al., 1989; Endo et al., 1989).

† This work was supported by grants from HFSP and the Ministry of Education of Japan.

* Correspondence should be addressed to this author.

0006-2960/92/0431-677$03.00/0

Epidermal growth factor (EGF)[1] is a peptide hormone that initiates a number of cellular responses by binding to specific receptors on the surface of target cells (Carpenter & Cohen, 1979). Mayo et al. (1987) have studied the interaction of EGF with micelles of sodium dodecyl sulfate (SDS) and dodecylphosphocholine (DPC) using photochemically induced dynamic nuclear polarization (CIDNP) ^{1}H NMR spectroscopy. Photo-CIDNP NMR spectroscopy is a technique used to identify solvent-exposed Tyr, Trp, and His residues in proteins (Kaptein, 1982). Its high sensitivity and selectivity to these aromatic rings make it possible to measure NMR spectra in the presence of a large excess of detergents. Mouse EGF contains five Tyr at residues 3, 10, 13, 29, and 37, two Trp at 49 and 50, and one His at 22 (Savage et al., 1973). Mayo et al. found that SDS and DPC micelles reduce the solvent accessibility of Tyr37, Trp49, and Trp50 and, to a lesser extent, that of Tyr10. They stated that the residues 37, 49, and 50 are involved in a major interaction site and that residue 10 represents a minor interaction site with micelles.

In the present study, we investigated the interaction of mEGF with detergent micelles by using the combination of two-dimensional ^{1}H NMR and perdeuterated DPC. The use of perdeuterated detergents is a key to eliminating the huge proton resonances from the detergent micelles and spin diffusion effects which obscure the quantitative analysis of NMR data (Brown, 1979). We assigned all the proton resonances of mEGF in the presence of DPC micelles at pH 6.8 by means of two-dimensional NMR and determined the three-dimensional structure of micelle-bound EGF. We found that the C-terminal tail[2] takes an amphiphilic structure as bound to DPC micelles.

Materials and Methods

EGF purified from submaxillary glands of adult male mice by chromatography on Bio-Gel P10 and DEAE-cellulose (Savage & Cohen, 1972) was further purified by reverse-phase HPLC (Kohda & Inagaki, 1988). Perdeuterated dodecylphosphocholine (DPC) was synthesized according to the method of Brown (1979). L-α-Dimyristoylphosphatidylcholine (PC, synthetic) and L-α-phosphatidylserine (PS, from bovine brain) were purchased from Sigma.

NMR Measurements. Mouse EGF samples were dissolved at 6 mM in 99.95% ^2H_2O or in 90% ^1H_2O/10% ^2H_2O with 40 mole ratio of perdeuterated DPC to EGF. The pH was adjusted to an uncorrected glass electrode reading of 6.8 using a Radiometer PHM86. No extra salt was added to the sample. Novel NMR microcell tubes with symmetric geometry purchased from Shigemi, Japan, was used to reduce the sample volume to 0.15 mL (Takahashi & Nagayama, 1988). ^{1}H NMR spectra were recorded on a 500-MHz JEOL JNM-GX500 spectrometer at a probe temperature of 28 °C. Sodium 2,2-dimethyl-2-silapentane-5-sulfonate (DSS) was added as an internal chemical shift standard. Because the DSS methyl group resonance is sharp at pH 6.8 in the absence of micelles, but broad and split in their presence, the chemical shifts are reported relative to a sharp peak from an impurity (0.152 ppm). DQF-COSY spectra (Rance et al., 1983), HOHAHA spectra (Bax & Davies, 1985), and NOESY spectra (Jeener et al., 1979; Macura et al., 1981) were recorded in the phase-sensitive mode (States et al., 1982). All two-dimensional spectra were recorded with 512 × 2048 data points and with a spectral width of 7000 Hz. HOHAHA spectra were recorded with a mixing time of 30 ms. NOESY spectra were recorded with mixing times of 80, 150, and 200 ms. The water resonance was suppressed by selective irradiation during the relaxation delay. For the measurement of NOESY, the water resonance was suppressed by means of the DANTE pulse (Zuiderweg et al., 1986) or jump–return pulse (Plateau & Gueron, 1982). A total of 64–128 scans were accumulated for each t_1, with a relaxation delay of 1.0 s. The digital resolution was 6.8 Hz/point in both dimensions with zero-filling in the t_1 dimension. A phase-shifted sine function was applied for both t_1 and t_2 dimensions in the case of DQF-COSY, and a Lorentz–Gauss function was applied in other cases.

Simulated Annealing Calculations. Energy minimization and molecular dynamics calculations were made using the program XPLOR (version 1.5, Polygen Corp., Waltham, MA) on a Silicon Graphics Iris 4D/70G. The three-dimensional structure of mEGF bound to DPC micelles was calculated by successive use of two XPLOR programs (Brünger, 1987) based on the simulated annealing (Nilges et al., 1988a) and variable target function method (Nilges et al., 1988b) as previously described (Lancelin et al., 1991). Analyses of calculated coordinates were carried out using XPLOR, and structures were displayed and plotted using the program QUANTA (version 3.1, Polygen).

Fluorescence Measurements. Tryptophan fluorescence was measured on a Hitachi MPF-4 spectrofluorometer by excitation at 295 nm (slit width 5 nm) and recording the emission spectra between 310 and 410 nm (slit width, 15 nm). Mouse EGF (3 μM in 40 mM potassium phosphate buffer, pH 7.0) was titrated by stepwise addition of DPC or phospholipid vesicles composed of pure PC (phosphatidylcholine) or PC/PS (phosphatidylserine) (1:1, mol/mol) prepared by tip sonication.

Results

Sequence-Specific Resonance Assignments at pH 6.8 in the Presence of DPC Micelles. The sequence-specific resonance assignments of mEGF in the presence of DPC micelles at pH 6.8 were made by comparison with the NMR spectra measured in the absence of DPC micelles at the same pH. The sequence-specific resonance assignments in the absence of DPC in pH 6.8 solution had been accomplished using the combination of a two-dimensional pH titration experiment (Kohda et al., 1991) and the sequential assignment method (Kohda & Inagaki, unpublished results). Most of the proton resonances barely shifted on addition of DPC, and their assignments are straightforward by visual inspection of DQF-COSY and HOHAHA spectra (data not shown). More than 80% resonances were readily assigned in this way. The assignments of the remaining resonances (residues 13, 35, 36, and 46–53) were completed by the sequential assignment method (Wüthrich, 1986). Figure 1 shows a NOESY spectrum with a 200-ms mixing time obtained from a sample in ^1H_2O. The resonances in the C-terminal tail were assigned unambiguously by the $d_{\alpha N}$ walk from Thr44 to Arg53. The sequential NOE connectivities and the chemical shift table containing a total of 266 proton resonances are available as supplementary material.

[1] Abbreviations: CIDNP, chemically induced dynamic nuclear polarization; DPC, dodecylphosphocholine; DQF-COSY, double-quantum-filtered correlation spectroscopy; EGF, epidermal growth factor; DSS, sodium 2,2-dimethyl-2-silapentane-5-sulfonate; mEGF, mouse EGF; hEGF, human EGF; HOHAHA, homonuclear Hartmann–Hahn spectroscopy; NOE, nuclear Overhauser effect; NOESY, NOE spectroscopy; PC, phosphatidylcholine; PS, phosphatidylserine; RMS, root mean square; RMSD, RMS deviation; SA, simulated annealing; SDS, sodium dodecyl sulfate; T_m, gel to liquid-crystalline phase transition temperature; VTF, variable target function.

[2] The "C-terminal tail" corresponds to the last eight residues, 46–53, of mouse EGF, while the "main core" means residues 1–45 in this paper. The amino acid sequence of mouse EGF is shown in Figure 2.

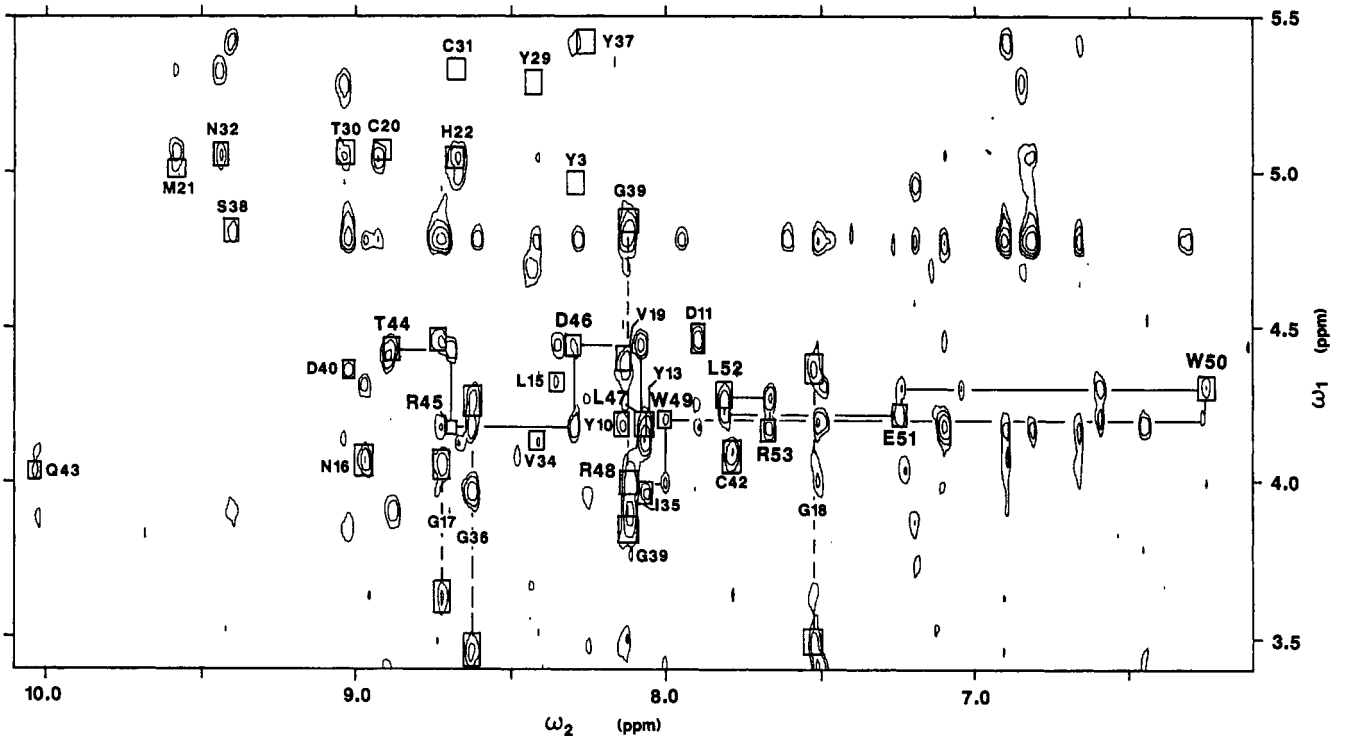

FIGURE 1: Fingerprint region of the NOESY spectrum (200-ms mixing time) of mouse EGF bound to perdeuterated dodecylphosphocholine micelles at pH 6.8 and 28 °C in ^1H_2O solution. The water signal was suppressed by a jump–return pulse. The positions of the COSY cross peaks are indicated by boxes. The cross peaks of L47 and Y13 are nearly overlapped. The two COSY cross peaks of a Gly residue are connected with a vertical broken line. A $d_{\alpha N}$ walk, T44–R45–D46–L47–R48–W49–W50–E51–L52–R53, is shown by horizontal and vertical solid lines with a break between L47 and R48 due to an accidental overlap with an intraresidue NOE of Y10.

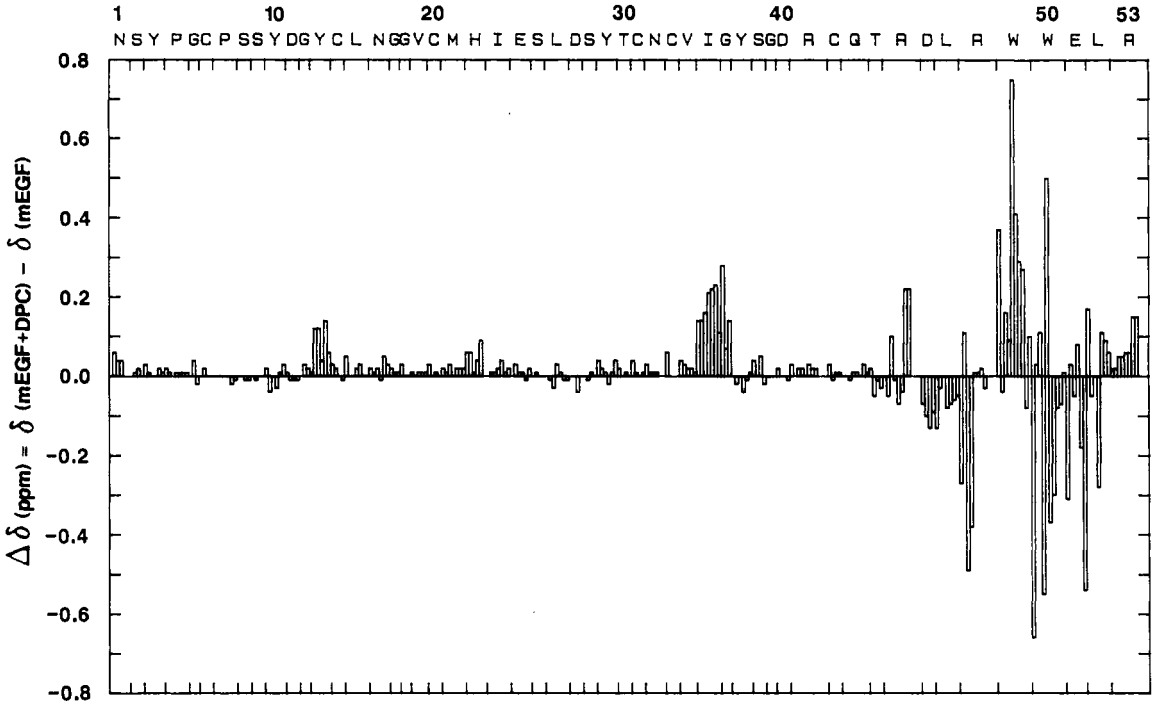

FIGURE 2: Comparison between the chemical shifts of the proton resonances of mEGF in the presence and absence of DPC micelles. All assigned proton resonances are aligned along the amino acid sequence and within residues in the following order: NH, $C^{\alpha}H$, $C^{\beta}H$, $C^{\gamma}H$, $C^{\delta}H$, ... Where either resonance of the two states of mEGF was not observed, no comparison was made and a space was inserted.

A comparison between the chemical shifts observed in the presence and absence of the DPC micelles is shown in Figure 2. Clearly the proton resonances of residues 46–53 were significantly shifted on addition of DPC, implying that these residues form a primary interaction site with DPC micelles. The proton resonances of Tyr13, Ile35, and Gly36 were also shifted. Since Ile35 and Gly36 are located near the C-terminal tail in acidic pH solutions without DPC (Montelione et al., 1987; Kohda et al., 1988), they are possibly involved in a part of the major binding site. On the other hand, Tyr13 is isolated in space from these affected residues. Probably Tyr13 is located in a minor interaction site pointed out by Mayo et al. (1987). Though their photo-CIDNP NMR experiments exhibited that Tyr10, not Tyr13, was a weak interaction site, these two Tyr residues are actually in contact in space.

Simulated Annealing Calculations. We collected inter-

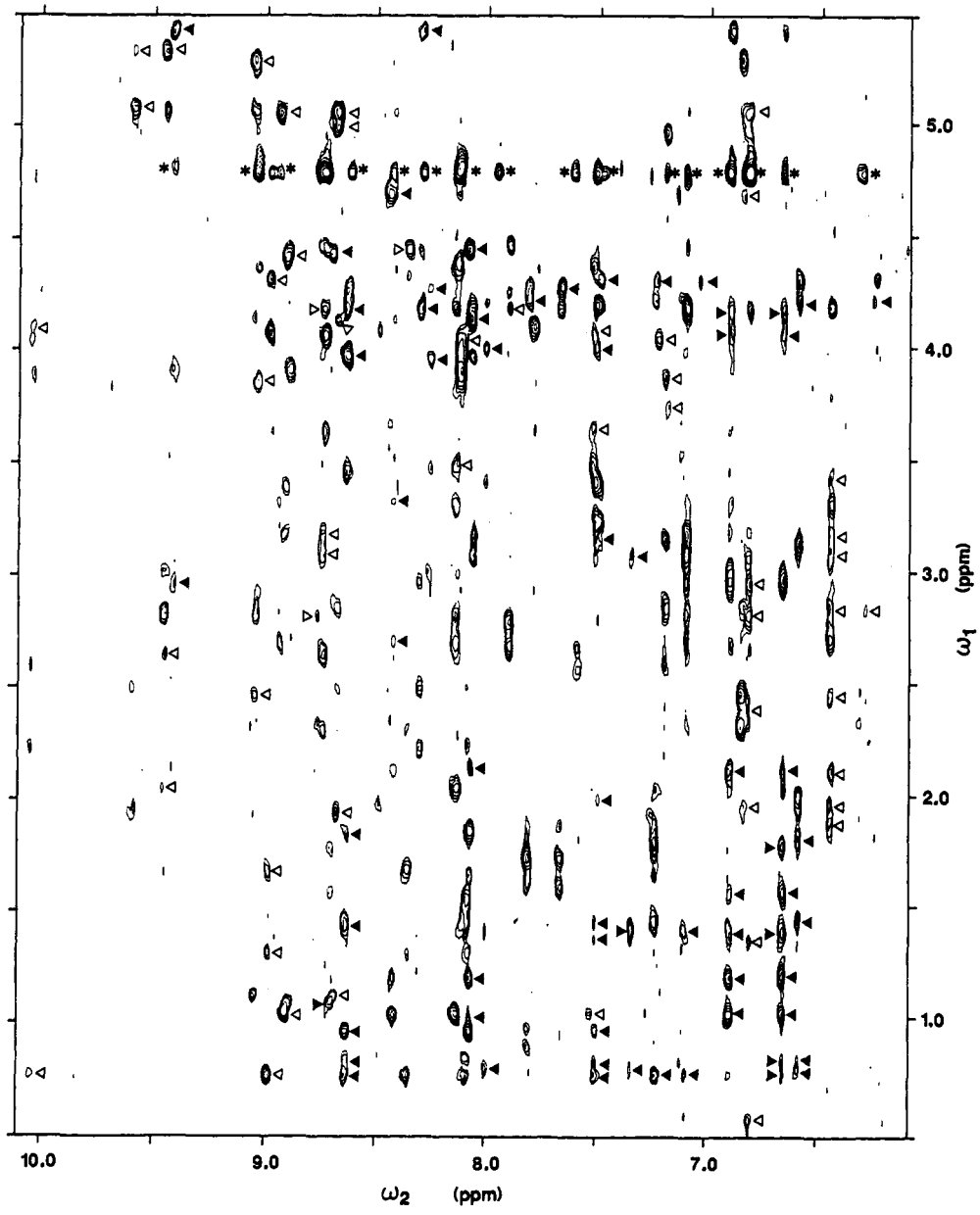

FIGURE 3: Spectral region (ω_1 = 0.5–5.5, ω_2 = 6.1–10.1 ppm) from the same NOESY spectrum as in Figure 1. Interresidue NOE cross peaks for determining the three-dimensional structure of the micelle-bound C-terminal portion of mEGF, that is, NOEs involving V34–Y37 or R45–R53, are marked by filled triangles, while the other interresidue NOE cross peaks are marked by open triangles. Artifactual cross peaks from the water signal are marked with asterisks. Other unmarked cross peaks are intraresidue NOEs or unassigned NOE peaks to a particular proton pair.

proton distances from NOESY spectra recorded in the presence of DPC micelles. Most NOEs were found to be identical for free and bound forms of mEGF (Figure 3, cross peaks marked by open triangles). The number of NOEs, however, was reduced due to broadening of the NMR resonances as bound to the micelles. Judging from chemical shift values and NOEs, the core of mEGF still maintains its three-dimensional structure when interacting with micelles. Since chemical shift values are a sensitive parameter for detecting conformational changes of proteins, the data presented in Figure 2 clearly indicate the structural similarity of the core in the absence and presence of DPC micelles. For example, the interstrand NOEs $d_{\alpha\alpha}$(2,23), $d_{\alpha\alpha}$(20,31), $d_{\alpha\alpha}$(22,29), and $d_{\alpha\alpha}$(37,45) indicate that mEGF bound to the micelles contains the identical antiparallel β-sheet structures. Many interdomain NOEs involving residues 13, 15, 16, and 18 in the N-terminal domain (1–32) and residues 37, 41, and 43 in the C-terminal domain (33–53) suggest a similar relative orientation of the two domains.

In the present study, we concentrate our attention on the major interaction site. Thus, we used the coordinates[3] of mEGF without DPC for the main core (residues 1–45) and an extended conformation for the C-terminal tail (residues 46–53) as a starting structure. Atomic positions of the residues 35, 36, and 46–53, whose chemical shifts were affected by DPC, were varied during calculations. In addition, the atoms on the residues 34, 37, and 45, located at the boundary between affected and unaffected residues, were also allowed to move. However, the atomic positions of the remaining residues were fixed to save computation time.

NOEs involving these residues (34–37 and 45–53) were selected and used as input to the XPLOR programs (Figure 3, cross peaks marked by filled triangles). The 17 sequential NOEs observed in a ^1H_2O NOESY experiment with a mixing

[3] The coordinates used for the main core were the mean structure of 10 converged XPLOR structures at pH 6.8 in the absence of micelles (unpublished data). The global conformation of mEGF at pH 6.8 is similar to that at pH 2.0.

time of 150 ms were divided into three groups with upper bound distance constraints of 2.8, 3.0, and 3.2 Å, considering from the lower limit (2.2 Å) and the upper limit (3.55 Å) of the distances for a $d_{\alpha N}$ connectivity (Wüthrich, 1986). They are rough estimates due to the relatively long mixing time and a rapid exchange of amide protons with solvent water. Tertiary NOEs (NOEs other than intraresidue and sequential NOEs) were collected from NOESY spectra obtained in ^2H_2O with mixing times of 80 and 200 ms and NOESY spectra obtained in ^1H_2O with a mixing time of 200 ms. The upper bound distance constraints for these 52 NOEs were set to fixed values of 4.0 Å for the 80-ms mixing time and 5.0 Å for the 200-ms mixing time to allow for the possible effects of spin diffusion. The lower bound distance constraints were set to 1.8 Å for all constraints. For cross peaks involving methyl groups, an additional 0.5 Å per methyl group was added to the upper bound distance constraints (Clore et al., 1987). A complete NOE list is available as supplementary material.

We used XPLOR to calculate the three-dimensional structure of micelle-bound mEGF. Our XPLOR procedure was composed of two stages, namely, a VTF stage and a SA stage (Lancelin et al., 1991). In the VTF step, the simulated annealing method based on a variable target function and a soft asymptotic NOE potential function was used (Nilges et al., 1988b). Initial velocities at 1000 K were assigned randomly to the floating atoms of a starting structure to introduce random sampling into the calculations. Pseudoatom corrections (Wüthrich, 1983) were added to the upper and lower bound distance constraints during this stage. A total of 69 distance constraints were entered. The structures obtained in the VTF stage were subsequently used as a starting structure for the SA stage (Nilges et al., 1988a). Distance constraints from hydrogen bonds (Val34 NH–Tyr37 CO and Val34 CO–Tyr37 NH) were added to the set of NOE constraints. The distances involving protons without stereospecific assignments are referred to $(\langle r^{-6}\rangle)^{-1/6}$ average distance so that no corrections were made.

Three-Dimensional Structure of Micelle-Bound mEGF. A total of 41 calculations were carried out starting from randomly assigned initial velocities. There were no violations greater than 0.5 Å for all the solutions. We chose 10 structures as judged by the criterion of smallest RMS violations. The selected structures had also smallest values of other energy terms. A mean structure was obtained by averaging the coordinates of the final structures which were first superposed to the best converged structure for a minimum pairwise RMSD of the backbone atoms (N, C^α, C′) for residues 34–37 and 45–50. The averaged coordinate was subsequently subjected to a restrained Powell minimization (Clore et al., 1986). The statistics of the XPLOR calculations are summarized in Table I. In Figure 4A, the backbone of the 10 structures has been superimposed with the mean structure for pairwise minimum RMSDs of the backbone atoms for residues 34–37 and 45–50. The average RMSD is 0.51 Å with a standard deviation of 0.14 Å. The backbone of the C-terminal tail takes an extended conformation in the presence of DPC. Six NOEs between Ile35/Gly36 and Leu47 determine the relative orientation of the C-terminal tail toward the main core (Figure 4B).

A superposition of the 10 XPLOR structures with side chains in the C-terminal tail region is shown in Figure 5. The 10 structures have been best fitted with the mean structure for pairwise minimum RMSDs of non-hydrogen atoms for residues 46–50. The average RMSD is 1.17 Å with a standard deviation of 0.23 Å. Clearly, the C-terminal tail adopts an amphiphilic structure. Hydrophobic side chains (Leu47, Trp49, Trp50, and Leu52 in thick lines) are aligned on one side and form a hydrophobic cluster, while charged residues (Asp46, Arg48, Glu51, and Arg53 in thin lines) are aligned on the other side. The lipid–water interface probably lies along the extended backbone of the C-terminal tail.

Table I: Structural Statistics[a]

	10 structures	mean structure
RMS deviations from experimental distance constraints (Å) (73)[b]	0.053 ± 0.008[c]	0.042[c]
F_{NOE} (kcal·mol^{-1})[d]	10.6 ± 3.3	6.4
F_{repel} (kcal·mol^{-1})[d]	33.8 ± 4.2	26.3
F_{dihed} (kcal·mol^{-1})[d]	7.3 ± 1.4	6.6
E_{L-J} (kcal·mol^{-1})[e]	−85.0 ± 8.4	−89.9
RMS deviations from idealized geometry[f]		
bond (Å) (807)	0.009 ± 0.0005	0.008
angle (Å) (1430)	2.83 ± 0.004	2.82
improper (deg) (289)[g]	0.442 ± 0.04	0.393

[a] The "10 structures" refers to the final set of XPLOR structures, the "mean structure" refers to the structure obtained by restrained minimization of the averaged coordinate of the individual 10 structures. The number of specified constrains are given in parentheses. [b] Includes four constraints for two hydrogen bonds. [c] No violations greater than 0.5 Å for the 10 structures and none greater than 0.2 Å for the mean structure. [d] The value of the square-well NOE potential F_{NOE} is calculated with a force constant of 50 kcal·mol^{-1}·Å^{-2}. The value of the repel term F_{repel} is calculated with a force constant of 4 kcal·mol^{-1}·Å^{-4} with the van der Waals radii scaled by a factor of 0.8 of the standard value used in the CHARMM empirical function (Brooks et al., 1983). The dihedral term F_{dihed} is used only to restrain the peptidic ω angle in trans with a force constant of 200 kcal·mol^{-1}. [e] E_{L-J} is the Lennard-Jones van der Waals energy calculated with the CHARMM empirical energy function (Brooks et al., 1983), which was not included in the simulated annealing calculations. [f] For all the residues of mEGF, although residues 1–33 and 38–44 were fixed during calculations. [g] The improper torsion term is used to maintain the planar geometries as well as the chiralities.

Fluorescence Measurements. Mouse EGF contains two Trp residues in the C-terminal tail. Thus the relative intensity and wavelength of maximum emission for the fluorescence of these Trp residues can be used as a specific indicator to investigate the interaction of the C-terminal tail with micelles or liposomes. A large increase in the intensity by a factor of more than 2 and a blue shift of 12 nm of the emission maximum were observed on addition of DPC (Figure 6). These changes occur above the critical micelle concentration of DPC (ca. 1 mM), indicating that the C-terminal tail does not interact with DPC monomers but with micelles, where two Trp residues penetrate into the micelles. As a binding model, we assume EGF + $DPC_n \rightleftharpoons$ EGF·DPC_n. The dissociation constant is equal to [EGF]·[DPC_n]/[EGF·DPC_n], where [EGF] is the free EGF concentration, [DPC_n] is the free DPC micelle concentration, and [EGF·DPC_n] is the concentration of the EGF-micelle complex. Assuming that $n = 40$ and that a 1:1 complex exists as in the cases of glucagon and melittin (Bösch et al., 1980; Lauterwein et al., 1979), the dissociation constant of mEGF and DPC micelles is about 0.1 mM at 28 °C and pH 7.0.

We investigated the interaction of mEGF with liposomes composed of PC or PC/PS (1:1, mol/mol) below and above T_m. Neither an increase in the intensity nor a blue shift was observed (data not shown). These observations indicate that mEGF does not interact with the lipid bilayer through the C-terminal tail.

Discussion

Sequence-specific resonance assignments of mEGF in the presence of perdeuterated DPC micelles were made (Figure 1). Then we collected interproton distances from the NOESY

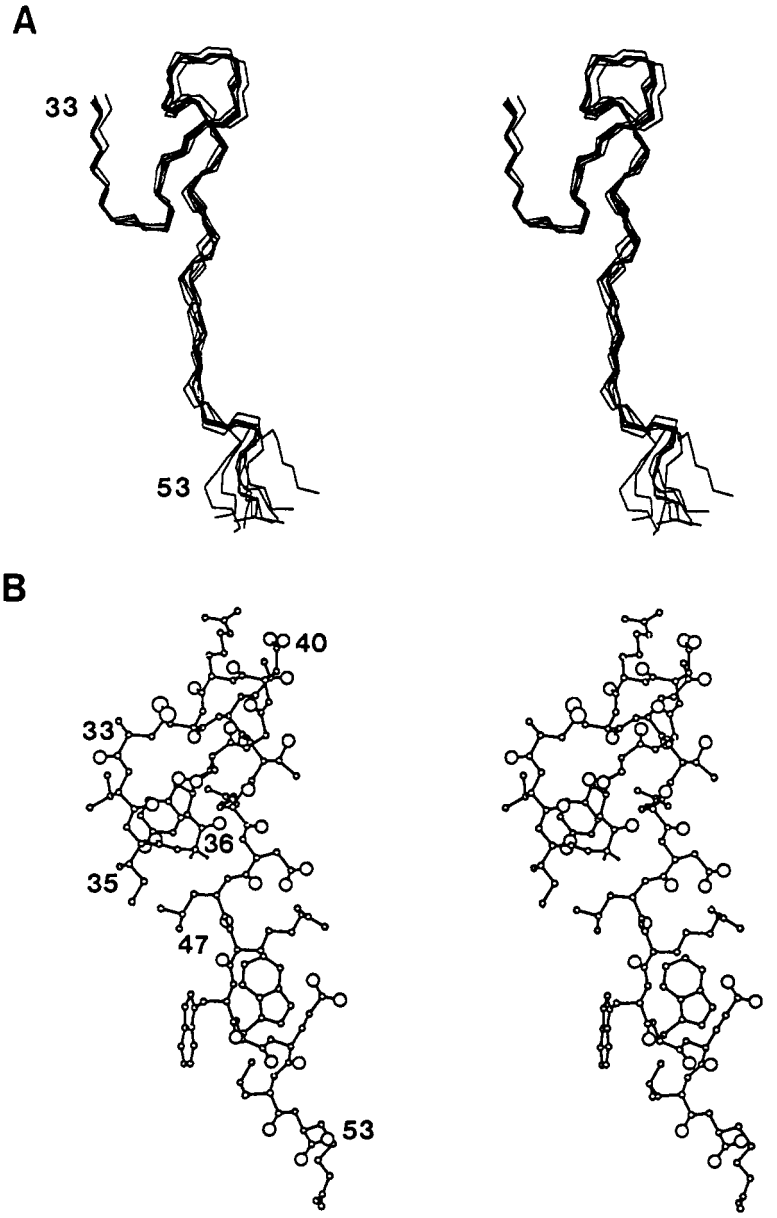

FIGURE 4: (A) Stereoview of a superposition of the backbone (N, C^{α}, C′) atoms (residues 33–53) of the 10 converged XPLOR structures of micelle-bound mEGF. The 10 structures have been best fitted with the mean structure for the backbone atoms of residues 34–37 and 45–50. The RMSD values are 0.51 ± 0.14 Å around the mean structure. (B) Stereoview of the mean structure showing the space arrangement of the side chains. Hydrogen atoms are omitted for clarity except for G36. One angstrom unit corresponds to 2.0 mm.

spectra recorded in the presence of perdeuterated DPC micelles (Figure 3) and calculated the three-dimensional structures of micelle-bound mEGF (Figures 4 and 5). Because the main core of mEGF maintained its conformation on the addition of DPC (Figures 2 and 3), only the atoms on residues 34–37 and 45–53 were allowed to move during simulated annealing calculations. The three-dimensional structure of the C-terminal tail is well defined (Figures 4 and 5) by using NOEs observed in the C-terminal region as bound to micelles. In the absence of micelles at pH 6.8, a part of the C-terminal tail, residue 46–50, takes a well-defined folded structure; and beyond residue 51, the conformation is less well defined owing to an insufficient number of NMR data (manuscript in preparation). By contrast, in the presence of micelles, the backbone of the C-terminal tail adopts an extended conformation which has an amphiphilic nature, suggesting that the interaction occurs at the lipid–water interface of DPC micelles.

The conformational change in the C-terminal region induced by micelles is confirmed by the chemical shift comparison between the native human EGF and a derivative lacking the C-terminal five residues, 49–53 (Cooke et al., 1990). The deletion of the C-terminal five residues influenced the chemical shifts of residues 35 and 36, in addition to residues 45–48. NOE data indicate that residues 35 and 36 are close to Trp49 and Trp50 in native hEGF (Cooke et al., 1990), and hence these residues are influenced by a large ring current effect from the Trp residues. The removal of Trp49 and Trp50 by the deletion caused the downfield shifts of the resonances of residues 35 and 36. Similar downfield shifts of these residues, in the case of mEGF bound to micelles, suggests that the two Trp residues move apart from residues 35 and 36 through a conformational change in the C-terminal region. Fluorescence experiments also demonstrated the DPC-induced conformational change. The intensity increase and blue shift of the fluorescence of Trp49 and Trp50 above the critical micelle concentration of DPC indicated that these Trp residues were embedded in a nonpolar environment inside micelles (Figure 6).

Since micellar systems are considered as models of membranes, we expected the same fluorescence changes on the

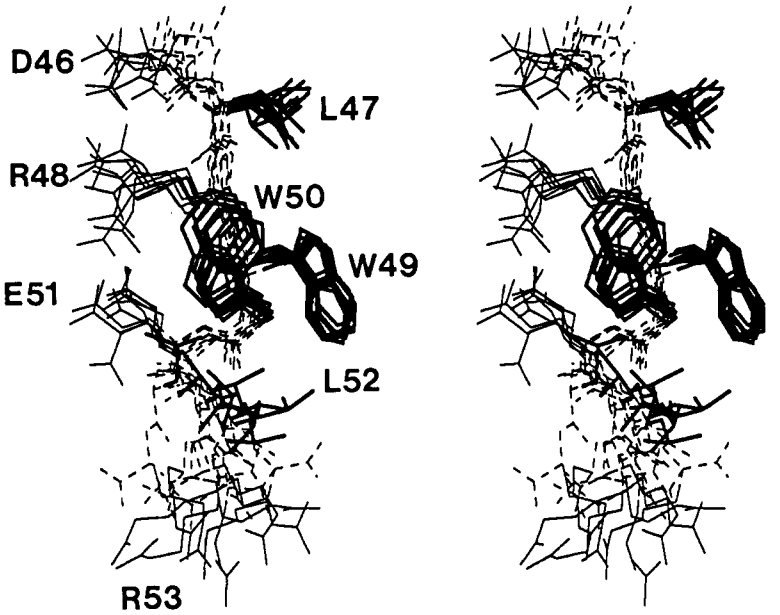

FIGURE 5: Stereoview of a superposition of the C-terminal tail (residues 46–53) of the 10 XPLOR structures of micelle-bound mEGF. The 10 structures have been best fitted with the mean structure of non-hydrogen atoms for residues 46–50. The RMSD values are 1.17 ± 0.23 Å around the mean structure. Hydrogen atoms are omitted for clarity. Hydrophobic residues (L47, W49, W50, and L52) are drawn in thick lines, hydrophilic residues (R45, D46, R48, E51, and R53) are in thin lines, and backbone atoms are in thin broken lines. One angstrom unit corresponds to 3.0 mm.

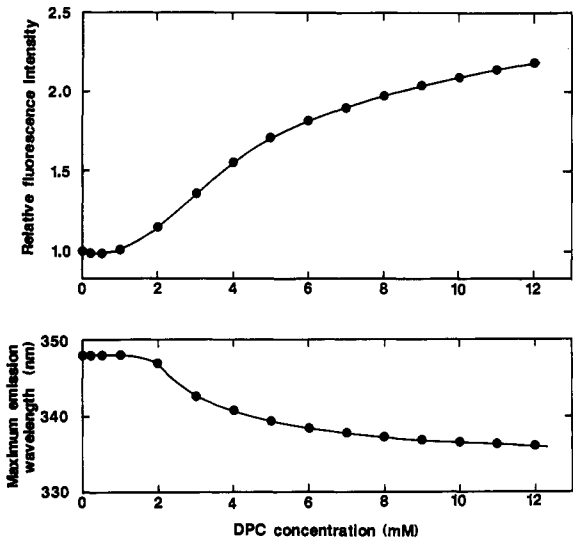

FIGURE 6: Relative intensity and wavelength of maximum emission of the fluorescence of Trp49 and Trp50 of mouse EGF as a function of added DPC concentration. Mouse EGF (3 μM) was in 40 mM potassium phosphate buffer, pH 7.0. The excitation wavelength was 295 nm, and the temperature was controlled at 28 °C. The critical micelle concentration of DPC is approximately 1 mM.

addition of vesicles composed of pure PC or a mixture of PC and PS (1:1, mol/mol). Neither an increase nor a shift of the fluorescence was observed below or above T_m. We therefore concluded that the micelles mimic a putative hydrophobic pocket on the receptor molecule rather than biomembranes. The C-terminal tail takes a unique conformation in the micelles, suggesting that it has an intrinsic propensity to form such a structure in a hydrophobic environment. An induced fit may occur in the C-terminal tail region on binding to the receptor. Greenfield et al. (1989) investigated the interaction of mEGF with the extracellular EGF binding domain of the EGF receptor. The Trp fluorescence maximum at 333 nm in the free receptor remained unchanged after the addition of mEGF (1:1, mol/mol). This finding means that the fluorescence maximum (346 nm) of the two Trp residues of mEGF in the free state changes to ca. 333 nm in the complex, suggesting that these Trp residues move into a nonpolar environment. In such an environment, the C-terminal tail changes its conformation as shown in the present study.

Leu47 is one of the strongly conserved amino acid residues among EGFs and EGF-like growth factors. For mouse EGF, the replacements of Leu47 by another amino acid residue exhibited reduced binding activity to the receptor (Ray et al., 1988). Similar results have been obtained for human EGF (Engler et al., 1988; Dudgeon et al., 1990; Matsunami et al., 1990) and human TGFα (Lazar et al., 1988). Interestingly, a type-conservative substitution, such as Leu47 to Val, resulted in a considerable reduction in receptor binding affinity (Ray et al., 1988; Dudgeon et al., 1990). A mutant of mEGF in which Leu47 was replaced by Ser was studied in detail by two-dimensional ^{1}H NMR (Moy et al., 1989). A chemical shift comparison between the proton resonances of the wild-type and the mutant suggested that conformational changes induced by the point mutation were only proximal to residue 47. Four Leu47 mutants of hEGF were also investigated by one-dimensional ^{1}H NMR (Dudgeon et al., 1990). Again the substitution of Leu47 had little effect on the protein structure. It is reasonable to conclude from these results that Leu47 is directly involved in the interaction with the receptors. It should be noted, however, that there is an implicit assumption: *The conformation of EGF does not change significantly upon binding to the receptor.* As was shown in the present study, however, the C-terminal tail containing Leu47 changes its conformation and adopts an amphiphilic structure in the presence of micelles. We would like to suggest that a similar conformational change occurs when EGF binds to the receptors. Leu47 may play a key role in the conformational change induced by receptor binding. The replacements of Leu47 by a hydrophilic residue, such as Asp, Glu, or Ser, will disturb the amphiphilic structure and hence reduce its receptor binding affinity. Even the replacements by another hydrophobic residue, Val or Ile, will inhibit the conformational change since these amino acids have a methyl group at C^β position. Probably appropriate contacts between Ile35/Gly36 and Leu47 may be necessary for completion of the conformational change

(Figure 5B). It is also possible that the side chain of Leu47 is directly recognized by the EGF receptor in the EGF–receptor complex after the conformational change. In this case, Leu47 has dual functions: a pivot of the conformational change and a contact residue. The hypothesis presented here explains the importance of Leu47 in receptor binding.

It was reported that the removal of the last five residues of mouse EGF did not influence either the receptor binding or in vitro mitogenic activity (Burgess et al., 1988). The segment Trp49–Trp50–Glu51–Leu52–Arg53 may help the conformation change around Leu47 described above by forming an amphiphilic structure at the hydrophobic pocket–water interface on the receptor. We infer that the conformational change around Leu47 can occur without the last five residues of EGF. The role of the last five residues is probably to control the kinetic properties of the EGF–receptor interaction, for example, enhancement of on and off rates through formation of the amphiphilic structure. Such changes in kinetic aspects may not be detected in the conventional assays of EGF.

In the present study, the lipid bilayers of liposomes did not induce the conformational change in mouse EGF characteristic of micelles. But, of course, we do not rule out the possibility of an interaction between the tail region of mEGF and lipid bilayers in an intermediate state before final binding to the receptor, considering the amphiphilic nature of the tail region.

Acknowledgments

We thank Dr. Iain D. Campbell of University of Oxford for fruitful discussion and critical reading of the manuscript.

Supplementary Material Available

One figure of the sequential NOE connectivities and two tables containing chemical shifts of mouse EGF at pH 6.8 in the presence of DPC micelles, distance constraints used in the calculations, and the coordinates (residues 33–53) for the mean structure of micelle-bound mEGF (13 pages). Ordering information is given on any current masthead page.

Registry No. EGF, 62229-50-9; DPC, 29557-51-5.

References

Bax, A., & Davis, D. G. (1985) *J. Magn. Reson. 65*, 393–402.
Bösch, C., Brown, L. R., & Wüthrich, K. (1980) *Biochim. Biophys. Acta 603*, 298–312.
Braun, W., Wider, G., Lee, K. H., & Wüthrich, K. (1983) *J. Mol. Biol. 169*, 921–948.
Brooks B. R., Bruccoleri, R. E., Olafson, B. D., States, D. J., Swaminathan, S., & Karplus, M. (1983) *J. Comput. Chem. 4*, 187–217.
Brown, L. R. (1979) *Biochim. Biophys. Acta 557*, 135–148.
Brown, L. R., Braun, W., Kumar, A., & Wüthrich, K. (1982) *Biophys. J. 37*, 319–328.
Brünger, A. T. (1988) XPLOR (version 1.5) manual, Polygen Corp.
Burgess, A. W., Lloyd, C. J., Smith, S., Stanley, E., Walker, F., Fabri, L., Simpson, R. J., & Nice, E. C. (1988) *Biochemistry 27*, 4977–4985.
Carpenter, G., & Cohen, S. (1979) *Annu. Rev. Biochem. 48*, 193–216.
Clore, G. M., Brünger, A. T., Karplus, M., & Gronenborn, A. M. (1986) *J. Mol. Biol. 191*, 523–551.
Clore, G. M., Nilges, M., & Ryan, C. A. (1987) *Biochemistry 26*, 8012–8023.
Cooke, R. M., Tappin, M. J., Campbell, I. D., Kohda, D., Miyake, T., Fuwa, T., Miyazawa, T., & Inagaki, F. (1990) *Eur. J. Biochem. 193*, 807–815.
Dudgeon, T. J., Cooke, R. M., Baron, M., Campbell, I. D., Edwards, R. M., & Fallon, A. (1990) *FEBS Lett. 261*, 392–396.
Endo, T., Shimada, I., Roise, D., & Inagaki, F. (1989) *J. Biochem. (Tokyo) 106*, 396–400.
Engler, D. A., Matsunami, R. K., Campion, S. R., Stringer, C. D., Stevens, A., & Niyogi, S. K. (1988) *J. Biol. Chem. 263*, 12384–12390.
Greenfield, C., Hiles, I., Waterfield, M. D., Federwisch, M., Wollmer, A., Blundell, T. L., & McDonald, N. (1989) *EMBO J. 8*, 4115–4123.
Inagaki, F., Shimada, I., Kawaguchi, K., Hirano, M., Terasawa, I., Ikura, T., & Go, N. (1989) *Biochemistry 28*, 5985–5991.
Jeener, J., Meier, B. H., Bachmann, P., & Ernst, R. R. (1979) *J. Chem. Phys. 71*, 4546–4553.
Kaptein, R. (1982) in *Biological Magnetic Resonance* (Berliner, L. J., & Reuben, J., Eds.) Vol. 4, pp 145–191, Plenum Publishing Corp., New York.
Kohda, D., & Inagaki, F. (1988) *J. Biochem. (Tokyo) 103*, 554–571.
Kohda, D., Go, N., Hayashi, K., & Inagaki, F. (1988) *J. Biochem. (Tokyo) 103*, 741–743.
Kohda, D., Sawada, T., & Inagaki, F. (1991) *Biochemistry 30*, 4896–4900.
Lancelin, J.-M., Kohda, D., Tate, S., Yanagawa, Y., Abe, T., Satake, M., & Inagaki, F. (1991) *Biochemistry 30*, 6908–6917.
Lauterwein, J., Bösch, C., Brown, L. R., & Wüthrich, K. (1979) *Biochim. Biophys. Acta 556*, 244–264.
Lazar, E., Watanabe, S., Dalton, S., & Sporn, M. B. (1988) *Mol. Cell. Biol. 8*, 1247–1252.
Macura, S., Huang, Y., Suter, D., & Ernst, R. R. (1981) *J. Magn. Reson. 43*, 259–281.
Matsunami, R. K., Campion, S. R., Niyogi, S. K., & Stevens, A. (1990) *FEBS Lett. 264*, 105–108.
Mayo, K. H., DeMarco, A., Menegatti, E., & Kaptein, R. (1987) *J. Biol. Chem. 262*, 14899–14904.
Montelione, G. T., Wüthrich, K., Nice, E. C., Burgess, A. W., & Scheraga, H. A. (1987) *Proc. Natl. Acad. Sci. U.S.A. 84*, 5226–5230.
Moy, F. J., Scheraga, H. A., Liu J.-F., Wu, R., & Montelione, G. T. (1989) *Proc. Natl. Acad. Sci. U.S.A. 86*, 9836–9840.
Nilges, M., Clore, G. M., & Gronenborn, A. M. (1988a) *FEBS Lett. 229*, 317–324.
Nilges, M., Gronenborn, A. M., Brünger, A. T., & Clore, G. M. (1988b) *Protein Eng. 2*, 27–38.
Olejniczak, E. T., Gampe, R. T., Rockway, T. W., & Fesik, S. W. (1988) *Biochemistry 27*, 7124–7131.
Plateau, P., & Gueron, M. (1982) *J. Am. Chem. Soc. 104*, 7310–7311.
Rance, M., Sørensen, O. W., Bodenhausen, G., Wagner, G., Ernst, R. R., & Wüthrich, K. (1983) *Biochem. Biophys. Res. Commun. 117*, 479–485.
Ray, P., Moy, F. J., Montelione, G. T., Liu, J.-F., Narang, S. A., Scheraga, H. A., & Wu, R. (1988) *Biochemistry 27*, 7289–7295.
Savage, C. R., Jr., & Cohen, S. (1972) *J. Biol. Chem. 247*, 7609–7611.
Savage, C. R., Jr., Hash, J. H., & Cohen, S. (1973) *J. Biol. Chem. 248*, 7669–7672.
States, D. J., Haberkorn, R. A., & Reuben, D. J. (1982) *J. Magn. Reson. 48*, 286–292.
Sui, S.-F., Urumow, T., & Sackmann, E. (1988) *Biochemistry 27*, 7463–7469.

Takahashi, S., & Nagayama, K. (1988) *J. Magn. Reson. 76*, 347-351.
Wüthrich, K. (1986) in *NMR of Proteins and Nucleic Acids* John Wiley, New York.
Wüthrich, K., Billeter, M., & Braun, W. (1983) *J. Mol. Biol. 169*, 949-961.
Zuiderweg, E. P. R., Hallenga, K., & Olejniczak, E. T. (1986) *J. Magn. Reson. 70*, 336-343.

Photoinduced Destabilization of Liposomes†

Henry Lamparski, Ulrich Liman, Judith A. Barry, David A. Frankel, V. Ramaswami, Michael F. Brown, and David F. O'Brien*

C. S. Marvel Laboratories, Department of Chemistry, University of Arizona, Tucson, Arizona 85721

Received July 15, 1991; Revised Manuscript Received October 11, 1991

ABSTRACT: The stability of two-component liposomes composed of the polymerizable 1,2-bis-[10-(2',4'-hexadienoyloxy)decanoyl]-*sn*-glycero-3-phosphatidylcholine (SorbPC) and either a phosphatidylethanolamine (PE) or a phosphatidylcholine (PC) were examined via fluorescence leakage assays. Ultraviolet light exposure of SorbPC-containing liposomes forms poly-SorbPC, which phase separates from the remaining monomeric lipids. If the nonpolymerizable lipids are PE's, then the photoinduced polymerization destabilizes the liposome with loss of aqueous contents. The permeability of the control dioleoylPC/SorbPC membranes was not affected by photopolymerization of SorbPC. The photodestabilization of dioleoylPE/SorbPC (3:1) liposomes required the presence of oligolamellar liposomes. NMR spectroscopy of extended bilayers of dioleoylPE/SorbPC (3:1) showed that the photopolymerization lowers the temperature for the appearance of ^{31}P NMR signals due to the formation of isotropically symmetric lipid structures. These observations suggest the following model for the photoinduced destabilization of liposomes composed of PE/SorbPC: photopolymerization induced phase separation with the formation of enriched domains of PE, which allows the close approach of apposed regions of enriched PE lamellae and permits the formation of an isotropically symmetric structure between the lamellae. The formation of such an interlamellar attachment (ILA) between the lamellae of an oligolamellar liposome provides a permeability pathway for the light-stimulated leakage of entrapped water-soluble reagents.

Several classes of biological lipids form hydrated membrane systems that display a variety of lamellar and nonlamellar phases as a function of temperature, pressure, and concentration. The formation of nonlamellar structures in membranes has been extensively investigated in recent years due to interest in their possible cell membrane role in the processes of fusion, endo- and exocytosis, and the transmembrane movement of large molecules [reviewed by Verkleij (1984), Cullis et al. (1985), Gruner et al. (1987), Hui (1988), Lindblom and Rilfors (1989), and Seddon (1990)].

Membranes composed of PE's, e.g., DOPE, are capable of forming inverted hexagonal (H_{II})[1] or inverted cubic (Q_{II}) phases. The H_{II} phase was first observed in the X-ray diffraction studies of Luzzati and co-workers in the 1960s (Luzzati & Reiss-Husson, 1962; Luzzati et al., 1968). It can also be detected by ^{31}P NMR (Cullis & de Kruijff, 1979) and ^{2}H NMR (Tilcock et al., 1982), by enhancement of the fluorescence intensity of lipid probes (Ellens et al., 1986a; Bentz et al., 1987; Hong et al., 1988), by differential scanning calorimetry (Van Dijck et al., 1976; Cullis & de Kruijff, 1978; Epand, 1985; Ellens et al., 1986a,b), and visualized by freeze-fracture electron microscopy (Deamer et al., 1970; Gulik-Krzywicki, 1975; Hui et al., 1981) as well as cryomicroscopy (Siegel et al., 1989a; Talmon et al., 1990).

Frequently a phase with isotropic symmetry (Luzzati & Reiss-Husson, 1962) is found between the lamellar and the hexagonal phases (Lindblom & Rilfors, 1989). In some instances it is observed only after the hydrated lipid sample is cycled several times through the temperature region of T_H (Shyamsunder et al., 1988; Veiro et al., 1990). Phospholipid membranes that show this metastable Q_{II} phase exhibit cubic X-ray diffraction patterns, isotropic ^{31}P NMR spectra (Cullis & de Kruijff, 1979; Hui et al., 1983), and lipidic particles in freeze-fracture electron microscopy images (Hui et al., 1981, 1983; Tilcock et al., 1982; Verkleij et al., 1982; Epand & Bottega, 1988). Ellens et al. (1986b) presented evidence that lipid membranes that exhibit isotropic structures are able to fuse with neighboring liposomes. Bentz et al. (1987) assert that lipid membranes that begin, but do not rapidly complete, the transition from lamellar to the hexagonal phase are likely to be fusion competent [see also Ellens et al. (1989) and Siegel et al. (1989b)].

PE liposomes are generally unstable at physiological pH unless they also consist of other lipids such as PC (Stollery & Vail, 1977). Processes which lead to the phase separation of PE and other lipids can trigger the lamellar to nonlamellar phase transition(s) (Ellens et al., 1984, 1986b; Conner et al.,

† This research was supported in part by a National Science Foundation Grant DMR-8722341 (D.F.O.), by a National Institutes Health Grant GM41413 (M.F.B.), by funds provided by the University of Arizona, and by a Deutsche Forschungsgemeinschaft fellowship (U.L.) and a National Institutes of Health postdoctoral fellowship (J.A.B.).

[1] Abbreviations: ANTS, 8-Aminonaphthalene-1,3,6-trisulfonic acid disodium salt; CHEMS, cholesteryl hemisuccinate; DMF, dimethylforamide; DOPC, dioleoylphosphatidylcholine; DOPE, dioleoylphosphatidylethanolamine; DOPE-Me, *N*-methylated dioleoylphosphatidylethanolamine; DPX, *p*-xylylenebispyridinium bromide; GPC, L-α-glycerophosphorylcholine; T_H, lamellar liquid-crystalline/hexagonal phase transition; H_{II}, inverted hexagonal phase; NMR, nuclear magnetic resonance; PE, phosphatidylethanolamine; Q_{II}, inverted cubic phase; SorbPC, 1,2-bis-[10-(2',4'-hexadienoyloxy)decanoyl]-*sn*-glycero-3-phosphatidylcholine; THF, tetrahydrofuran; TES, *N*-[Tris(hydroxymethyl)-methyl]-2-aminoethanesulfonic acid; TPE, PE prepared from egg phosphatidylcholine by transphosphatidylation.

0006-2960/92/0431-685$03.00/0